

Received February 13, 2020, accepted February 21, 2020, date of publication February 28, 2020, date of current version March 11, 2020.

Digital Object Identifier 10.1109/ACCESS.2020.2977163

A Controllable DCCS-Based PT Temperature Sensor in High Precision Molecular Spectroscopy Application

GUANGXIANG YANG^{1,2} AND YUANRONG WEN²

¹Chongqing Engineering Laboratory for Detection, Control and Integrated System, Chongqing Technology and Business University, Chongqing 400067, China

²School of Computer Science and Information Engineering, Chongqing Technology and Business University, Chongqing 400067, China

Corresponding author: Guangxiang Yang (ygxmonkey@126.com)

This work was supported in part by the Chongqing Science and Technology Bureau, China, under Grant cstc2019jcsx-msxmX0007, and cstc2015jcyjA90003, and in part by the Chongqing Education Committee Cooperation Foundation, China, under Grant KJ1500620.

ABSTRACT In the high precision molecular spectroscopy, the temperature of gas absorption cell is accurately measured. In this paper we discuss the factors affecting the measurement accuracy of temperature sensor employing platinum resistance in a resonant quartz crystal tuning fork (QCTF) detector based wavelength modulation spectroscopy (WMS). A bridge temperature sensor powered by a dual constant current source (DCCS) is proposed. The DCCS was controlled to keep the constant current of 1mA in this work. Furthermore, we used the 3-wire measurements powered by DCCS to eliminate the impact of lead resistances and self heating of the platinum resistance so as to reduce measurement errors. A piecewise linearization model by linear approximation algorithm is employed to evaluate the measurement calibration and increase the measurement accuracy. Detection of trace methane (CH₄) was demonstrated using a near infrared distributed feedback diode laser near 1.653 μm and a single pass gas absorption cell with an optical length of 20 cm. An example of the temperature sensor employing Pt100 with 3-wire measurement is developed in the detection of CH₄ with the temperature range from 0°C to 100°C. The controllable DCCS method is demonstrated by the measurement results of the deploying Pt100 sensors. Experimental results show that the accuracy of our proposed temperature sensor is improved in comparison with the conventional platinum resistance thermometer. The measurement accuracy is relatively increased due to employing the piecewise linear approximation model. The results also show good performance for measurement calibration, especially for high temperature region.

INDEX TERMS Temperature measurement, wavelength modulation spectroscopy, controllable dual constant current source, platinum resistance, piecewise linear approximation.

I. INTRODUCTION

Atmospheric methane (CH₄) is a significant greenhouse gas which may have a great influence on atmospheric compositions and climate [1]. Furthermore, CH₄ is also known as an industrial safety hazard and a variety of techniques have been presented for CH₄ detection. Among these detection technologies, a standard quartz crystal tuning fork (QCTF) was proposed [2], [3], which converts an optical signal into an electrical signal via quartz piezoelectric properties. The temperature measurement requirement is an essential parameter in CH₄ detection technology. The accuracy of temperature

may have an important impact on CH₄ detection results. High accuracy temperature measurement is also widely applied in many industrial and scientific applications such as solar radiation environments [4], ocean temperature measurements [5], Prognostics and health management [6], intelligent manufacturing [7], industrial process [8], agriculture monitoring and machinery fault diagnosis applications [9]. It is desirable to measure temperature with high precision in an industrial temperature range (−40°C and +85°C) and an extended temperature range (−40°C and +125°C) in various areas.

Platinum resistance [10], [11] with high precision, wide temperature sensing range and stable performance, has been applied to civil, industrial, military and other fields. In some applications of the limited requirements for measurement

The associate editor coordinating the review of this manuscript and approving it for publication was Mauro Fadda.

accuracy and temperature range, platinum resistances can be used with its linear characteristics. But in some fields with wider measurement range and higher accuracy (e.g. $\pm 0.1^\circ\text{C}$), the conventional platinum resistance temperature transducer is hard to be qualified. For example, in the sterilization of drug production, the measurement accuracy worse than $\pm 0.1^\circ\text{C}$ will have a serious influence on the quality of the drug [12]. In the process of the crystal growth, the temperature precision control is rigorous [13]. It is desirable to measure the temperature precisely by transducers, in particular for specific industrial fields. There are lots of work aiming to construct the high precision temperature sensors. Sanyal *et al.* [14] proposed a novel non-linear analog signal conditioning circuit for correcting the transfer curves of constant temperature anemometers. An improved lead resistance compensation technique for the 3-wire resistance temperature detectors was presented by Pradhan and Sen [15]. A new lead wire compensation technique was presented for conventional two wire resistance temperature detectors (RTDs) by Sen [16]. Minardo *et al.* proposed a temperature measurement by dual wavelength Brillouin sensors [17]. Chakraborty *et al.* presented a simple temperature measurement and transmission system of an electric heater operated in water bath [18]. Sarma and Boruah designed a high precision thermometer with the conditioned signal linearised using a 9th order polynomial and a 12-bit analog-to-digital converter and a 8-bit microcontroller for industrial application [19]. The technique of linearization of Pt sensors has been used and published in instrument industries such as Analog Device, Maxim, and Microchip [20]–[22]. Measurement accuracy of most of the products can't reach $\pm 0.1^\circ\text{C}$ according to the investigation on the current platinum resistance temperature transducer in the market. A four-wire electrical configuration was used to eliminate the effects of contact resistance and increase measurement accuracy by Shen *et al.* [23]. Zhang and Chen presented the relevant analysis and demonstrates the potential benefits of an integrated circuit solution to Johnson noise thermometry (ICJNTs) [24]. McDaniel *et al.* presented a dynamic, double ended calibration routine in response to site-specific challenges and constraints for calibration considerations [25]. A temperature measurement was developed in a single pass glass absorption cell with a length of 20 cm by Ma *et al.* [26]. Chuanliang *et al.* used technique for trace gas detection by tunable diode laser absorption spectroscopy, in which the spectral signals at different pressures and temperatures were acquired [27]. A laser sensor for trace ammonia (NH_3) was developed by Xinqian *et al.*, which was based on near-infrared laser absorption spectroscopy and a multipass cell with variable temperature is adopted [28].

In this paper, we proposed a temperature measurement technique with a controllable dual constant current source by using platinum resistance for high accuracy temperature sensing in a QCTF based methane detection. This temperature sensing is used in a high sensitivity QCTF based wavelength modulation spectroscopy. A controllable DCCS sensor is equipped on the gas cell of methane detection. As for a

basic characteristic of each measurement result, it needs to be calibrated and evaluated [29]. We employed a piecewise linear approximation model for calibration of measurement and reducing the measurement error in accordance with the application requirements. The comparison between simplified cut-off linearization model and piecewise linear approximation model, during a case study for platinum resistance calibration is illustrated.

II. MEASUREMENT ERRORS ANALYSIS

The temperature measurement by utilizing platinum resistance may produce errors because of the environment influence and measurement methodology [30], [31]. In order to lower the errors of temperature sensor, we discuss and analyze the measurement methodology herein.

The accuracy, reliability and consistency of the sensor are unavoidable because of manufacturing error. Besides, the non-linear characteristics of platinum resistance, wires of sensors, lead resistances, quantization error [32] and the other errors associated with thermoelectric effects and amplifier offsets may have an influence on measurement results.

A. NON-LINEAR CHARACTERISTICS OF PLATINUM RESISTANCE

The general function for the industrial platinum resistance is defined as [33]:

$$R_t = R_0[1 + at + bt^2 + c(t - 100)t^3](-200^\circ\text{C} < t < 0^\circ\text{C}) \quad (1)$$

$$R_t = R_0[1 + at + bt^2](0^\circ\text{C} < t < 850^\circ\text{C}) \quad (2)$$

where,

t: temperature to be measured;

R_t: resistance at temperature t;

R₀ = 25.5359, resistance at 0°C or 0.001°C;

a = 3.9083 × 10⁻³;

b = -5.775 × 10⁻⁷;

c = -4.183 × 10⁻¹².

It is clear that platinum resistance itself has non-linear characteristics. As the coefficients b and c are very small (10^{-7} and 10^{-12}), they are omitted in many applications of small temperature range and low accuracy of measurement. The simplified linear equation (it is called cut-off linearity equation) is given by:

$$R_t = R_0[1 + at](0^\circ\text{C} < t < 850^\circ\text{C}) \quad (3)$$

Software or hardware methods are often used to compensate for the non-linear characteristics of platinum resistance. The measurement accuracy will be seriously lowered when platinum resistance is used as a linear element. The computing result of platinum resistance with non-linear characteristics at the range of 0°C~300°C is shown in Fig.1.

In this Figure, line 1 in blue is the computing result of platinum resistance by the equation (2). Line 2 in green is the result of platinum resistance with the simplified linear characteristics by equation (3). There is a deviation between

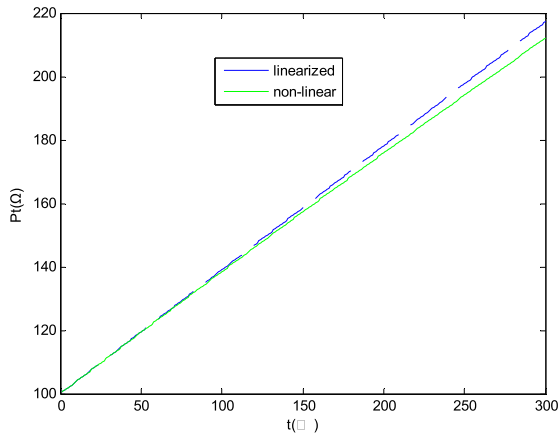


FIGURE 1. Computing result of platinum resistance with non-linear characteristics.

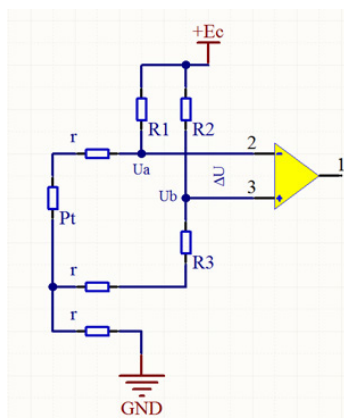


FIGURE 2. Constant voltage source based conditioning circuit.

line 1 and line 2. The maximum error of about 13°C occurs at 300°C.

B. NON-LINEAR CHARACTERISTICS OF SIGNAL CONDITIONING CIRCUIT

The platinum resistance temperature sensor transforms temperature change into that of resistance. Then the change of resistance is transformed into a proportional voltage or current variation by a signal conditioning circuit. In addition, the conditioning circuit will be responsible for the span and bring the nonlinear error to the measurement. There are two types of conditioning circuit which are constant voltage source and constant current source.

Constant voltage source based conditioning circuit is illustrated in Fig.2.

Pt is a platinum resistance of which value will change with temperature. A 3-wire measurement is connected in this diagram to eliminate the influence of lead wire resistances r. For simplification, it is assumed that r = 0. In the circuit, the bridge has a constant voltage +Ec power supply. The output of the constant voltage circuit bridge is derived as follows:

$$\begin{aligned} \Delta u &= u_a - u_b = \frac{P_t}{(P_t + R_1)} E_c - \frac{R_3}{(R_2 + R_3)} E_c \\ &= \frac{P_t R_2 - R_1 R_3}{(P_t + R_1)(R_2 + R_3)} E_c \end{aligned} \tag{4}$$

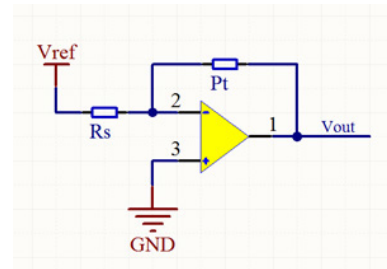


FIGURE 3. Constant current source based conditioning circuit.

The output of circuit is nonlinear according to the equation (4). Consequently, the constant voltage source based conditioning circuit will produce nonlinear error to the temperature measurement. In some applications of low accuracy requirements, equation (4) is usually simplified as:

$$\Delta u = \left(\frac{P_t}{R_1} - \frac{R_3}{R_2} \right) E_c \tag{5}$$

Constant current source based conditioning circuit is presented in Fig.3.

In the figure, Pt is a platinum resistance; Vref is a reference voltage; Rs is a sampling resistance. The output of the circuit is determined by the following equation.

$$V_{out} = - \frac{V_{ref}}{R_s} P_t \tag{6}$$

The output of platinum resistance using DCCS is linear from this equation. But the constant current source circuit can not eliminate the error of lead resistance caused by using 3-wire measurements. Furthermore, the output of the circuit can not become zero due to the influence of ambient temperature [34]. Therefore the constant current source based conditioning circuit is rarely used in the field application.

C. DRIFTS AND FLUCTUATIONS OF RESISTANCE

The temperature signals acquired by resistance will go through a signal conditioning circuit, an amplifier and an analog to digital (A/D) converter. The characteristics of various electronic devices may change with time and temperature. Thus inaccuracy and uncertainty of temperature measurement will be caused by the drift [35], [36] or/and fluctuation. The measurement results are frequently compensated and calibrated by means of resistance’s zero point output, thermal zero shift, full-scale output etc. Also the measurement errors may include other factors such as thermoelectric effects, amplifier offsets and self heating of the resistance.

D. QUANTIZATION ERROR

The quantization error [37], [38] in the measurement is unavoidably caused by the digital methodology. The error is mainly from A/D converting and signal processing. It is one of the factors which may reduce the measurement accuracy.

III. METHODOLOGIES

A. A CONTROLLABLE DCCS BASED MEASUREMENT

It is mentioned previously that the measurement is influenced by lead resistances in constant voltage source based

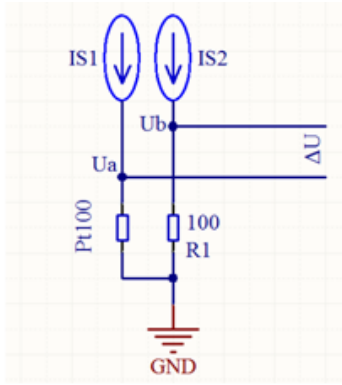


FIGURE 4. Framework of dual constant current source.

conditioning circuit with 3-wire measurements. This is because that the lead resistance is eliminated on condition of the same current flowing on two bridge arms. However it is difficult to keep the same current on two bridge arms in constant voltage current conditioning circuit. Once the temperature changes, the current will vary with the platinum resistance. Therefore the measurement accuracy is reduced.

Within this work we proposed a controllable DCCS method using 3-wire measurements to eliminate the influence of lead resistances and drifts. The 3-wire measurements diagram is shown in Fig.2. Resistance r is the lead resistance. Three wires are with the same characteristics, sizes and the same resistances value r . The platinum resistance Pt is 100 ohms when the measured temperature is 0°C. The resistance $R3$ is equal to 100 ohms. Usually $R1$ is equal to $R2$, the two bridge arms have the same current. As a result, the voltage difference ΔU between Ua and Ub is zero.

The proposed framework of two bridge arms powered by controllable dual constant current source is shown in Fig.4. In order to eliminate the effect lead resistance, two bridge arms are powered by two constant current sources $IS1$ and $IS2$ respectively. In order to keep the current on two bridge arms to be equal, the $IS1$ and $IS2$ are controllable. The basic characteristics of the constant current source is that the output current $IS1$ and $IS2$ are kept constant when the load changes. The Pt100 platinum resistance will change with the temperature changes. As two constant current sources $IS1$ and $IS2$ are kept same, the current flowing through the bridge arm will not change. Therefore it is able to eliminate effect of platinum resistance on the measuring accuracy caused by lead resistance.

The output ΔU of the bridge is derived by Eq.(6):

$$\Delta U = PtIS_1 - R_1IS_2 \tag{7}$$

Assuming $IS_1 = IS_2 = IS$, we have:

$$\Delta U = (Pt - R_1)IS \tag{8}$$

It is a linear output of bridge according to Eq.(8). By means of this method, the error created by non-linearity is eliminated. Actually the constant current is set to 1mA, which is benefit for reducing the influence of temperature drift

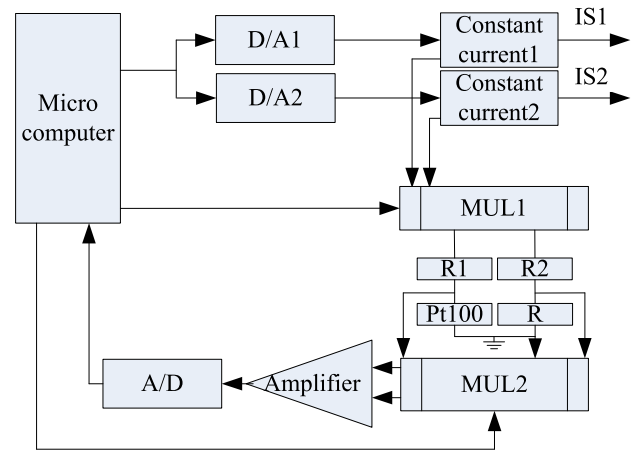


FIGURE 5. Controllable dual constant current source.

caused by current self-heating of the platinum resistance. The controllable dual constant current source design framework is shown in Fig.5.

In this figure, two constant currents are decided by two outputs voltage of DA1 and DA2 converter respectively which are controlled by a micro computer. The two outputs $IS1$ and $IS2$ of constant currents source flow through bridge arms constructed by $R1$, $R2$, $Pt100$ and R under the control of multiplexer $MUL1$. The voltage difference of bridge and voltage of R are input to a differential amplifier controlled by multiplexer $MUL2$. The output of AD converter is received by a micor computer and is used to compute the result of measured temperature. Besides, the output of AD converter rectifies the tow constant current sources outputs which are kept the same to 1mA by DA1 and DA2.

If $IS1$ is not equal to $IS2$, the micro computer will drive D/A converter to output a new value to amplifier to keep the equal output. Hence the voltage on lead resistance of platinum resistance is invariable. In this way, the output currents of two constant current sources are controlled and maintained to 1mA by the micro computer.

The conventional Pt100 thermometer with 3-wire measurement can only compensate the lead resistance of the Pt100 at a specific temperature (for example 0°C). Once the temperature changes, the currents flowing through two bridge arms will not be equal if the resistance of the Pt100 changes. The Pt100 lead resistance may lower measurement accuracy due to incomplete compensation. In this case it is difficult to achieve a high accuracy measurement. The developed temperature sensor is shown in Fig.6.

B. PIECEWISE LINEAR APPROXIMATION MODEL

The defined function for the industrial platinum resistance belongs to a non-linear model. In industry practice, the equation of platinum resistance is commomly linearized to computer processing. The linearization is often achieved near inflection points in the temperature response curve by an approximation function. A piecewise linear approximation model connects a number of linear segment functions to



FIGURE 6. The designed temperature sensor using DCCS.

better approximate the nonlinear platinum resistance transfer function. The linearization is that make resistance value as a linear function of temperature. The linearization model may lower the accuracy of measurement result compared with the original non-linear model. Three methods including feedback method, function transform method and function approach method are popular for calibrating the nonlinearity of platinum resistance. With these methods, the measurement result of sensor is calibrated and transformed to digital result. In this paper, we employ a typical piecewise linear approximation model for reducing the measurement error in accordance with the application requirements. The utilization of piecewise linear approximation model is illustrated in Fig.7. Curve A is the nonlinear function of platinum resistance. Line B is the ideal linearization model. Pt_0 , Pt_2 , Pt_m are platinum resistances at temperature of t_0 , t_2 and t_m , respectively.

It is assumed that the measured temperature range is from lowerT to upperT. A linearization function is set to approximate the response curve of platinum resistance from lowerT to upperT. In the response curve, the resistance pt_m of middle point temperature t_m is computed to find the corresponding temperature t_1 in linearization function B. These points are computed as follows:

$$Pt_2 = 100 * (1 + c_1 * t_2 + c_2 * t_2^2) \tag{9}$$

$$t_m = t_0 + (t_2 - t_0) / 2 \tag{10}$$

$$Pt_m = Pt_0 + (Pt_2 - Pt_0) / 2 \tag{11}$$

$$t_1 = (t_2 - t_0) / (Pt_2 - Pt_0) * (Pt_m - Pt_0) + t_0 \tag{12}$$

If the difference between t_m and t_1 is higher than desired error value (ERR), the upperT is lowered in response curve A and a new linearization function C is setup. Each time the gap of lowered upperT is called a step. The approaching is

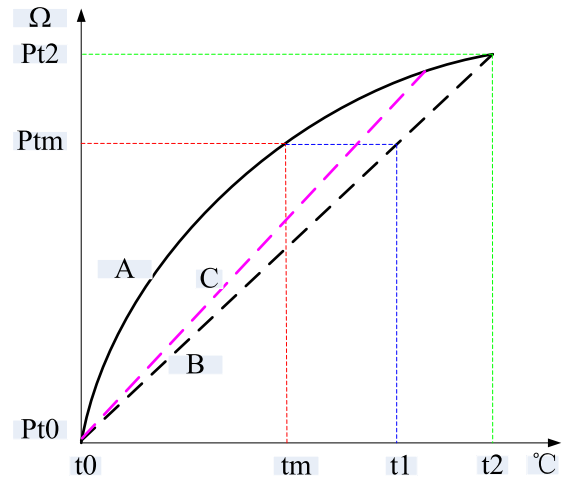


FIGURE 7. Piecewise linear approximation model.

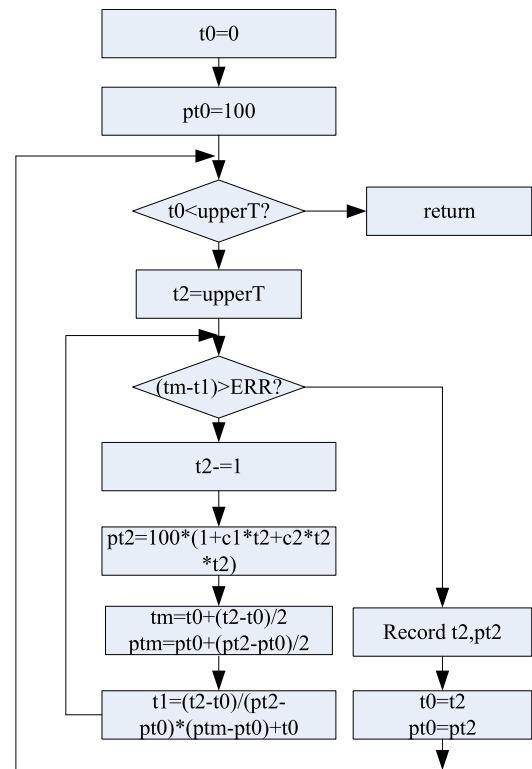


FIGURE 8. Flow chart of piecewise linear approximation model.

put forward step by step. When the searching point arrived the final point upperT, piecewise linear approximation completes. The flow chart of piecewise linear approximation model is illustrated in Fig.8.

IV. EXPERIMENTS AND RESULTS

The measurement technique has been calibrated using 4 thermometers. Water is used as a measured object in the experiment because of its large heat capacity and slow change of temperature, which can reduce the error produced by the reading time difference. As we know that standard thermometers are extremely delicate instruments; shock, vibration or

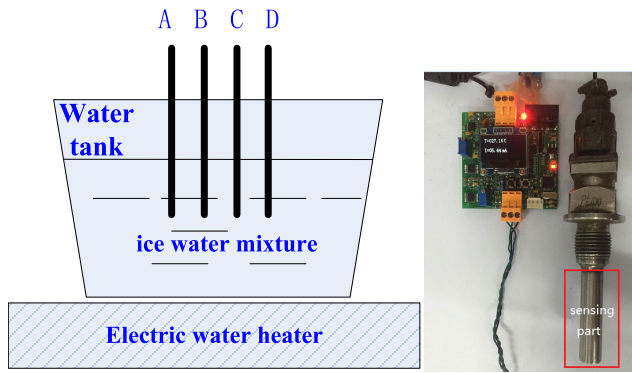


FIGURE 9. Four kinds of thermometer A,B,C and D.

any acceleration that causes the wire to flex will strain the wire and change its resistance. In this work, the temperature of ice-water mixture in a water tank is measured from 0°C to heated to boiling 100°C by using a Standard Mercury-in-Glass Thermometer (Grade I) (SMGT-I) as the standard calibrated thermometer A with an rated nominal accuracy of 0.01°C. A digital thermometer C with nominal accuracy of 0.1°C purchased from the market is used as a contrastive sample. A conventional Pt100 thermometer D with 3-wire measurement is designed in this work, which is compared with a controllable DCCS thermometer B. In order to investigate the temperature and thermal effects, all sensors in the experiments were exposed to an open environment in the research laboratory (average room temperature: 25.5±0.5°C; average relative humidity: 44 ± 3% RH; under a standard pressure of 101.325 Pa). In the heating process from 0°C to 100°C, both thermometer A, C and the designed temperature measurement sensor B, D are placed into the water tank. The sensing part of each sensors is put into the water tank so as to sense the temperature directly and accurately. The distance of four sensors in the water tank is less than 5cm, in order to minimize the measurement error. The water was heated by an electric water heater from outside the tank, as shown in Fig.9. In order to make the water has the same temperature in the tank, the water is perfectly stirred. Notice that the fixed point water in triple point of water is prepared by means of liquid-nitrogen as coolant. The measurement results of sensors are compared with A to compute the measurement error.

The ice water mixture is slowly heated to boiling with total time of about 30min. This was done very slowly, so that the temperature in the probe volume of sensors was the same as that measured by 4 thermometers. The readings of 4 thermometers A, B, C and D are recorded. The liquid is stirred at a constant speed to ensure that the ice water mixture is evenly heated. Repeating 10 times, the average of each reading is recorded, and then calculate the error between A and B,C,D respectively. We choose 6 tested points from 0°C to 100°C. The accuracy of the developed sensor B in this work is evaluated by two major indicators: The Average Error (AE) and the Mean squared Error (MSE) [39]. The average error is

TABLE 1. Measurement results of A,B and C.

N o	Readings of B(°C)	Readings of C(°C)	Readings of A(°C)	Errors of A and C(°C)	Errors of A and B(°C)
1	0.16	0.22	0.00	0.22	0.16
2	20.12	19.26	20.00	0.74	0.12
3	40.13	40.61	40.00	0.61	0.13
4	49.88	50.33	50.00	0.33	0.12
5	80.12	80.42	80.00	0.42	0.12
6	98.76	99.01	98.57	0.44	0.19

the average absolute value error between measured and real temperature of six testing points chosen from 0°C to 100°C. The average error AE is given as follows:

$$AE = \frac{1}{n} \sum_{i=0}^{n-1} |a_i - f_i| \tag{13}$$

MSE gives an overall idea of the errors which occurred during forecasting and measures the average squared deviation of predicted values from the real data. Its mathematical expression is as follows:

$$MSE = \frac{1}{n} \sum_{i=0}^{n-1} (a_i - f_i)^2 \tag{14}$$

where a_i corresponds to the real temperature value at point i , f_i represents the measured value and n is the total number of points constituting the temperature series.

The experimental results are shown in Table.1.

In order to clearly reveal the error of proposed measurement system B in this paper, a comparison is listed. The readings of A,B and C are listed and the errors of them are given. It can be seen that the errors of the sensor B proposed in this paper is much lower than that of the sensor C purchased from the market. Moreover, Table.1 shows a comparison between a common commercial sensor measured and real temperature and it is shown that the measured temperature of B is much closer to the real temperature. In this way, the errors of B and D are also computed and listed.

According to Table.1, the AE of B is 0.14, which is much lower than that of C (0.46). The MSE of B and C is 0.0203 and 0.2411, respectively. The measurement errors of B and C, B and D are shown in Fig.10.

This figure shows the curve of the measurement errors of B and C. Notice that the AE error of B is clearly smaller and more stable than that of C.

The measurement errors of conventional Pt100 thermometer D is also shown in Fig.10. From this figure, we can see that the measurement error of B is smaller and more stable than that of D.

This may be caused by the effects that both the platinum resistance and lead resistance will change with temperature, which make the current changed on two arms of a conventional 3-wire measurement. The current flowing through the arms of conventional 3-wire measurement is powered by a constant DC and is not controllable, which is mentioned in subsection 2.2. The conventional 3-wire connection method

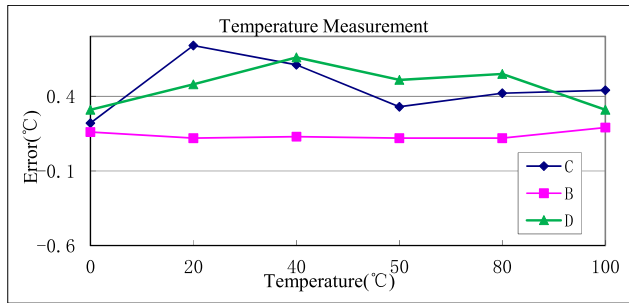


FIGURE 10. Measurement errors of thermometer B, C and D.

TABLE 2. MEasurement results of sensor B and D.

T(°C)	Readings of B(°C)	Readings of D(°C)	Readings of A(°C)	Errors of A and D(°C)	Errors of A and B(°C)
0	0.11	0.31	0	0.31	0.11
20	20.15	20.48	20	0.48	0.15
40	40.09	39.34	40	0.66	0.09
50	49.88	49.49	50	0.51	0.12
80	80.16	80.55	80	0.55	0.16
100	98.72	98.56	98.87	0.31	0.15

can not completely compensate for effect of the lead resistance in the full temperature range [7]. The temperature change may lead to zero point and full range drifting. These drifts have a great influence on the accuracy of temperature sensor.

Furthermore, as mentioned in Fig.2, the conventional constant-voltage conditioning circuit will bring nonlinear error to Pt 100 sensor. In order to avoid the temperature rising caused by the bridge arm current flowing through PT100 and lower the temperature measurement accuracy in most PT100 based temperature measurement applications, the current flowing through the bridge arm should be strictly limited. In this work, it is less than 5mA. The resistance values of R1 and R2 in figure 2 usually reach thousands of ohms. To ensure that when the temperature is 0 °C and the bridge output is 0V, the value of R3 is determined as 100 ohms. For the simplified design, the relationship between the simplified bridge output and PT100 resistance is linear, which ignores the non-linear error caused by the conditioning current of Pt100 sensor. The temperature accuracy of the constant-voltage PT100 temperature conditioning circuit is difficult to reach ± 0.1 °C. In view of the non-linear error caused by the constant-voltage 3-wire conditioning circuit of Pt100 temperature sensor, a new constant-current conditioning circuit without non-linear error is proposed. We have made some experiments of proposed new constant-current 3-wire sensor B which are compared with the conventional constant-voltage and 3-wire sensor D. The experimental results is shown in the Table 2.

According to this table, we can see that the average measurement errors of B is much less than that of D. It means that the DCCS based thermometer B can effectively avoid the temperature rising caused by the bridge arm current flowing

TABLE 3. Piecewise linear approximation (PLA) results.

N	Range of T (°C)	Range of Pt C(°C)	Error(°C)	PLA function
1	0.0 ≤ T < 36.0	100.000~113.995	0.0481	$t=2.572341*(pt-100.0)+0.0$
2	36.0 ≤ T < 72.0	113.995~127.840	0.0487	$t=2.600151*(pt-113.995036)+36.0$
3	72.0 ≤ T < 100.0	127.840~138.505	0.0297	$t=2.625382*(pt-127.840384)+72.0$

TABLE 4. Comparisons of linearity equation (L) and the segmentation Linearity model (PLA).

Temperature(°C)	Err of L(°C)	Err of PLA(°C)	Results of L(°C)	Results of PLA(°C)
0	0	0	0	0
18	0.0484	0.0481	18.0484	18.0481
36	0.1945	0.0027	36.1945	36.0027
54	0.44	0.0487	54.44	54.0487
72	0.7865	0.0004	72.7865	72.0004
86	1.127	0.0297	87.127	86.0297
100	1.5304	0.0015	101.5304	100.0015

through PT100. Besides, thermometer B is able to reduce the non-linear error caused by the constant-voltage 3-wire conditioning circuit of Pt100 temperature sensor D. So the measurement accuracy can be improved.

In the experiment, a piecewise linear approximation model is proposed to reduce the error. The linear approaching functions from 0°C to 100°C are computed and listed as Table.2:

According to Table 3, we can see that the temperature function is divided into 3 segmentations from 0°C to 100°C. Approaching functions are different with the temperature range of 36°C,72°C,100°C, respectively. Each approaching function is given in light of measurement accuracy which is 0.1°C.

The computed results of the simplified cut off linearity equation (L) and piecewise linear approximation model (PLA) are listed in Table 4. In this table, it is shown that the errors of L become higher with the temperature rising. The maximum error is 1.5304°C at 100°C. On the contrary, the errors of PLA are very small in comparison with L and are fallen within the range of ± 0.1 °C. The maximum errors are located in the middle of three approaching functions which are 18°C, 54°C and 86°C, respectively.

The error comparison of L and PLA is clearly shown in Fig.11.

To estimate the accuracy of DCCS based sensors, we conduct the experiment which compares the sensor of ordinary constant voltage source based conditioning circuit and 3-wire measurements with the sensor employing DCCS. As is mentioned previously that the measurement accuracy may be decreased by lead resistances in constant voltage source based conditioning circuit with 3-wire measurements. We use an ordinary constant voltage source sensor Sa and a DCCS based sensor Sd as two samples. Both sensors' measurement results

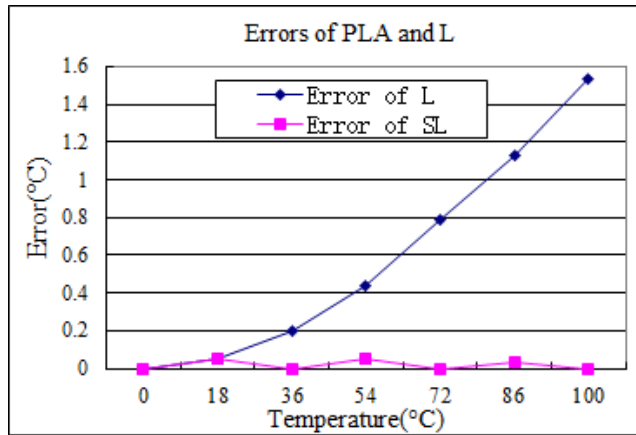


FIGURE 11. Error comparison of L and PLA.

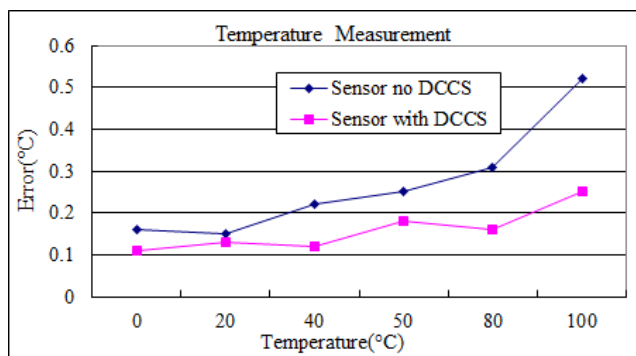


FIGURE 12. Sensor errors comparison between DCCS and no DCCS.

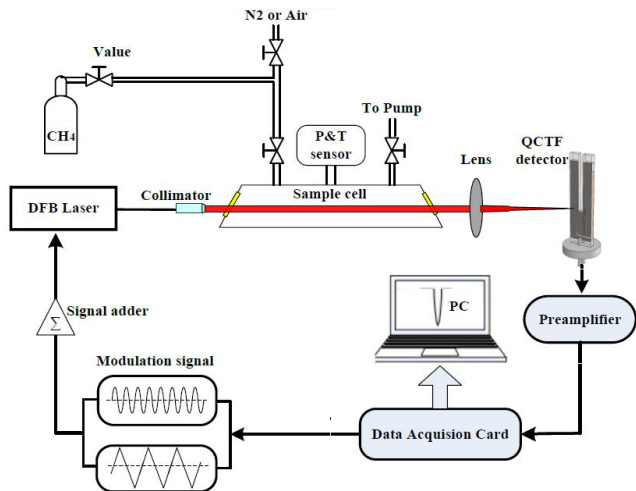


FIGURE 13. Schematic configuration of the CH₄ sensor system with DCCS based sensor.

are compared with a Standard Mercury-in-Glass Thermometer (Grade I) and the same experiment condition with that of in Fig.9. The results and the measurement uncertainties are addressed in Fig.12.

This developed DCCS based sensor is applied in a resonant QCTF detector based wavelength modulation spectroscopy. A schematic diagram of the experimental setup is presented in Figure 13. A fiber-coupled distributed feedback (DFB) diode laser emitting at 1653 nm is used as the excitation

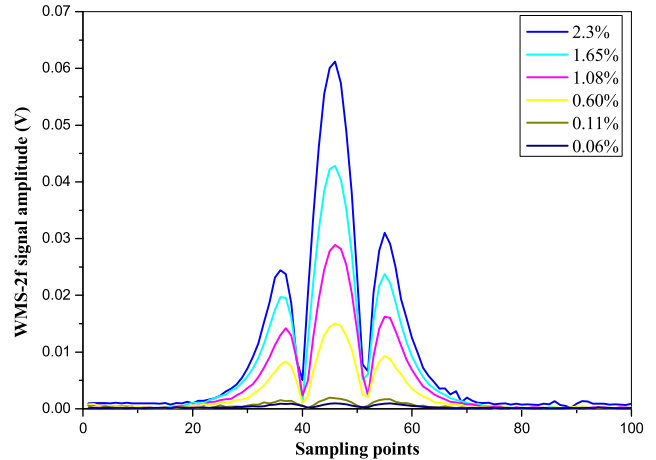


FIGURE 14. Experimentally measured WMS-2f signals under different CH₄ mixing ratio.

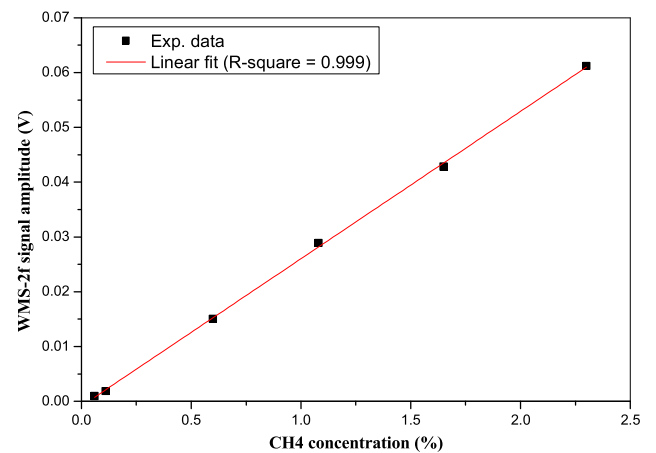


FIGURE 15. Linearity of the measured WMS-2f signal peak amplitudes and CH₄ mixing ratio.

light source for targeting the R₃ of the 2ν₃ band of CH₄ near 6046.95 cm⁻¹. The laser beam is collimated by a fiber collimator and directed to a single pass glass absorption cell with a length of 20 cm. The gas cell is equipped with a DCCS based temperature sensor and a pressure gauge and two CaF₂ windows with apertures of 25 mm for entrance and exit of the laser beam. After transmitted from the gas cell, the laser light was focused on the QCTF detector by an optical lens (CaF₂, focal length f = 25 cm).

To verify the linear concentration response of the sensor system, a series of CH₄ samples were made and the measured WMS-2f spectra with different CH₄ mixing ratio are shown in Figure 14. The measured 2f signal peak amplitude as a function of the CH₄ concentration and the linear fit are shown in Figure 15. Linear regression leads to a regression coefficient R² of 0.999 was obtained, the good linearity shows a good agreement with the theoretical expectation.

V. CONCLUSION

It is demonstrated a high accuracy temperature measurement method implemented by a dual constant current source based conditioning circuit. The DCCS is used as a standard

power source in order to compensate the lead resistance and temperature drift of sensors, which is difficult to be achieved by conventional constant-voltage 3-wire measurements. A piecewise linear approximation model is employed for calibration of measurement and reducing the measurement error in advanced industry applications such as trace gas detection by laser absorption spectroscopy. The proposed DCCS sensor, which uses a dual constant current conditioning circuit, is able to eliminate the non-linear error caused by the conventional constant-voltage conditioning circuit of Pt100 temperature sensor. Therefore, the proposed precise temperature measurements can be performed in a much wider temperature range by DCCS and piecewise linear approximation model, instead of 4-wire measurements. Based on the present study, it can be expected that the method could be extended to other measurements such as pressure, so that the applicability of the technique could be further improved in the future. It is also demonstrated by experiments with 4 samples that this technique can improve the measurement accuracy to $\pm 0.1^\circ\text{C}$ FS within the range of 0°C to 100°C . By using piecewise linear approximation model, the calibration of measurements is evaluated and validated.

ACKNOWLEDGMENT

The authors thank the Chongqing Lexu Electrical Company for the experiments provided by X. Liu and Y. Liu. They also thank Prof. J. Li for his help in this work.

REFERENCES

- [1] S. Park, J. C. Thomas, K. W. Brown, and K. Sung, "The use of biofilter to reduce atmospheric global warming gas (CH_4) emissions from landfills," *Int. J. Control*, vol. 6, no. 4, pp. 337–342, Dec. 2001.
- [2] J. Sun, H. Deng, N. Liu, H. Wang, B. Yu, and J. Li, "Mid-infrared gas absorption sensor based on a broadband external cavity quantum cascade laser," *Rev. Sci. Instrum.*, vol. 87, no. 12, Dec. 2016, Art. no. 123101.
- [3] J. Ding, T. He, S. Zhou, L. Zhang, and J. Li, "Quartz tuning fork-based photodetector for mid-infrared laser spectroscopy," *Appl. Phys. B, Lasers Opt.*, vol. 124, no. 5, pp. 9–78, Apr. 2018.
- [4] J. Ballestrín and M.-I. Roldán, "Contact sensors for measuring high surface temperature in concentrated solar radiation environments," *Measurement*, vol. 109, pp. 65–73, Oct. 2017.
- [5] J. Díaz-Álvarez, A. Tapetado, C. Vázquez, and H. Miguélez, "Temperature measurement and numerical prediction in machining Inconel 718," *Sensors*, vol. 17, no. 7, p. 1531, Jun. 2017.
- [6] D. Wang, F. Yang, Y. Zhao, and K.-L. Tsui, "Prognostics of lithium-ion batteries based on state space modeling with heterogeneous noise variances," *Microelectron. Rel.*, vol. 75, pp. 1–8, Aug. 2017.
- [7] A. DeMario, P. Lopez, E. Plewka, R. Wix, H. Xia, E. Zamora, D. Gessler, and A. Yalin, "Water plume temperature measurements by an unmanned aerial system (UAS)," *Sensors*, vol. 17, no. 2, p. 306, Feb. 2017.
- [8] M. Lindner, E. Tunc, K. Werneck, F. Heilmeier, W. Volk, M. Jakobi, A. W. Koch, and J. Roths, "Regenerated Bragg grating sensor array for temperature measurements during an aluminum casting process," *IEEE Sensors J.*, vol. 18, no. 13, pp. 5352–5360, Jul. 2018.
- [9] F. Mezzadri, F. C. Janzen, G. Martelli, J. Canning, K. Cook, and C. Martelli, "Optical-fiber sensor network deployed for temperature measurement of large diesel engine," *IEEE Sensors J.*, vol. 18, no. 9, pp. 3654–3660, May 2018.
- [10] R. Palenčár, P. Sopkuliak, J. Palenčár, S. Ďuriš, E. Suroviak, and M. Halaj, "Application of Monte Carlo method for evaluation of uncertainties of ITS-90 by standard platinum resistance thermometer," *Meas. Sci. Rev.*, vol. 17, no. 3, pp. 108–116, Jun. 2017.
- [11] G. Keshavaditya, G. R. Eranna, and G. Eranna, "PRT embedded microheaters for optimum temperature distribution of air-suspended structures for gas sensor applications," *IEEE Sensors J.*, vol. 15, no. 7, pp. 4137–4140, Jul. 2015.
- [12] A. Ancona, "Progress in the sterilization of drugs without heat," *Bollettino Chimico Farmaceutico*, vol. 93, no. 7, p. 251, 1954.
- [13] R. Niewa, D. Rau, A. Wosylus, K. Meier, M. Hanfland, M. Wessel, R. Dronskowski, D. A. Dzivenko, R. Riedel, and U. Schwarz, "High-pressure, high-temperature single-crystal growth, *ab initio* electronic structure calculations, and equation of state of $\epsilon\text{-Fe}_3\text{N}_{1+x}$," *Chem. Mater.*, vol. 21, no. 2, pp. 392–398, Jan. 2009.
- [14] N. Sanyal, B. Bhattacharyya, and S. Munshi, "An analog non-linear signal conditioning circuit for constant temperature anemometer," *Measurement*, vol. 39, no. 4, pp. 308–311, May 2006.
- [15] S. Pradhan and S. Sen, "An improved lead compensation technique for three-wire resistance temperature detectors," *IEEE Trans. Instrum. Meas.*, vol. 48, no. 5, pp. 903–905, 1999.
- [16] S. K. Sen, "An improved lead wire compensation technique for conventional two wire resistance temperature detectors (RTDs)," *Measurement*, vol. 39, no. 5, pp. 477–480, Jun. 2006.
- [17] A. Minardo, A. Coscetta, E. Catalano, and L. Zeni, "Simultaneous strain and temperature measurements by dual wavelength Brillouin sensors," *IEEE Sensors J.*, vol. 17, no. 12, pp. 3714–3719, Jun. 2017.
- [18] S. Chakraborty, S. K. Bera, S. C. Bera, and N. Mandal, "Design of a simple temperature transmitter circuit of an electric heater operated water bath," *IEEE Sensors J.*, vol. 18, no. 8, pp. 3140–3151, Apr. 2018.
- [19] U. Sarma and P. K. Boruah, "Design and development of a high precision thermocouple based smart industrial thermometer with on line linearisation and data logging feature," *Measurement*, vol. 43, no. 10, pp. 1589–1594, Dec. 2010.
- [20] M. Looney, "RTD interfacing and linearization using an ADuC706x microcontroller," Analog Devices, Norwood, MA, USA, Appl. Note AN-0970, Jan. 2010, pp. 1–16.
- [21] S. Mirza, "High-accuracy temperature measurements call for platinum resistance temperature detectors (PRTDs) and precision delta-sigma ADCs," Dgu Mitteilungen Nachrichten, Maxim Integr. Products Appl. Note 4875, 2011. [Online]. Available: <http://eprints.qut.edu.au/17113/>
- [22] J. Day and S. Bible, "Piecewise linear interpolation on PIC12/14/16 series microcontrollers," Microchip Technol. Inc., Chandler, AZ, USA, Tech. Rep. Microchip AN942, Jan. 2005.
- [23] A. Shen, S. B. Kim, C. Bailey, A. W. K. Ma, and S. Dardona, "Direct write fabrication of platinum-based thick-film resistive temperature detectors," *IEEE Sensors J.*, vol. 18, no. 22, pp. 9105–9111, Nov. 2018.
- [24] X. Zhang and D. Chen, "An integrated circuit solution to Johnson noise thermometry using low-cost and fast CMOS technology," *IEEE Sensors J.*, vol. 19, no. 9, pp. 3240–3251, May 2019.
- [25] A. McDaniel, J. M. Tinjum, D. J. Hart, and D. Fratta, "Dynamic calibration for permanent distributed temperature sensing networks," *IEEE Sensors J.*, vol. 18, no. 6, pp. 2342–2352, Mar. 2018.
- [26] H. Ma, S. Qin, L. Wang, G. Wang, X. Zhao, and E. Ding, "The study on methane sensing with high-temperature low-power CMOS compatible silicon microheater," *Sens. Actuators B, Chem.*, vol. 244, pp. 17–23, Jun. 2017.
- [27] C. Li, X. Guo, W. Ji, J. Wei, X. Qiu, and W. Ma, "Etalon fringe removal of tunable diode laser multi-pass spectroscopy by wavelet transforms," *Opt. Quantum Electron.*, vol. 50, no. 7, p. 275, Jun. 2018, doi: [10.1007/s11082-018-1539-4](https://doi.org/10.1007/s11082-018-1539-4).
- [28] X. Guo, F. Zheng, C. Li, X. Yang, N. Li, S. Liu, J. Wei, X. Qiu, and Q. He, "A portable sensor for *in-situ* measurement of ammonia based on near-infrared laser absorption spectroscopy," *Opt. Lasers Eng.*, vol. 115, pp. 243–248, Apr. 2019, doi: [10.1016/j.optlaseng.2018.12.005](https://doi.org/10.1016/j.optlaseng.2018.12.005).
- [29] K. Shahanaghi and P. Nakhjiri, "A new optimized uncertainty evaluation applied to the monte-carlo simulation in platinum resistance thermometer calibration," *Measurement*, vol. 43, no. 7, pp. 901–911, Aug. 2010.
- [30] T. Müller, G. Grünefeld, and V. Beushausen, "High-precision measurement of the temperature of methanol and ethanol droplets using spontaneous Raman scattering," *Appl. Phys. B, Lasers Opt.*, vol. 70, no. 1, pp. 155–158, Jan. 2000.
- [31] N.-W. Moon and Y.-H. Kim, "Optimized thermal compensation method using clustering and drifted response stability for total power radiometer calibration," *IEEE Sensors J.*, vol. 17, no. 5, pp. 1269–1276, Mar. 2017.
- [32] L. Cai, Y. Zhao, and X.-G. Li, "A fiber ring cavity laser sensor for refractive index and temperature measurement with core-offset modal interferometer as tunable filter," *Sens. Actuators B, Chem.*, vol. 242, pp. 673–678, Apr. 2017.

- [33] J. V. Nicholas and D. R. White, *Traceable Temperatures*. Hoboken, NJ, USA: Wiley, 2001.
- [34] Y.-X. Guo, Z.-B. Shao, H.-B. Tao, K.-L. Xu, and T. Li, "Dimension-reduced analog-digital mixed measurement method of inductive proximity sensor," *Sensors*, vol. 17, no. 7, pp. 1533:1-1533:24, Jun. 2017.
- [35] M. Le Menn, "Calibration and temperature correction of a V-block refractometer," *Meas. Sci. Technol.*, vol. 29, no. 3, Feb. 2018, Art. no. 037001.
- [36] Y. Liu and T. Ma, "Parasitic resistance-based high precision capacitive MEMS accelerometer phase shift and its usage for temperature compensation," *IEEE Sensors J.*, vol. 18, no. 2, pp. 629-634, Jan. 2018.
- [37] Priyadarshi, R. Jaiswal, R. C. Nair, N. K. Yarlagadda, A. A. K. Senapati, and P. Mulage, "Adaptive gyroscope drift compensation based on temporal noise modelling," in *Proc. Int. Conf. Microelectron., Comput. Commun. (MicroCom)*, Jan. 2016, pp. 23-25.
- [38] J. Li, B. Yu, and H. Fischer, "Wavelet transform based on the optimal wavelet pairs for tunable diode laser absorption spectroscopy signal processing," *Appl. Spectrosc.*, vol. 69, no. 4, pp. 496-506, Apr. 2015.
- [39] R. Yang, M. A. P. Pertijs, and S. Nihtianov, "A precision capacitance-to-digital converter with 16.7-bit ENOB and 7.5-ppm/°C thermal drift," *IEEE J. Solid-State Circuits*, vol. 52, no. 11, pp. 3018-3031, Nov. 2017.



GUANGXIANG YANG received the B.S. and M.S. degrees in mechanical engineering and the Ph.D. degree in mechanical design and theory from the Wuhan University of Technology, Wuhan, China, in 1997, 2000, and 2005, respectively.

From 2006 to 2015, he was an Associate Professor with the School of Computer Science and Information Engineering, Chongqing Technology and Business University. He has been a Professor, since 2015. His research interests include intelligent control technology, wireless sensor networks and application, smart sensing and measurement, and industry automation.

YUANRONG WEN received the B.S. degree in industry automation from Yuzhou University, Chongqing, in 1983.

From 1983 to 2002, he was a Research Assistant with Yuzhou University. He has been a Lecturer with Chongqing Technology and Business University, since 2002. His research interests include electrical engineering, embedded system design, and computer integrated systems.

• • •